Zensei: Embedded, Multi-electrode Bioimpedance Sensing for Implicit, Ubiquitous User Recognition

Munehiko Sato[1][*] **Rohan S. Puri**[1] **Alex Olwal**[1][†] **Yosuke Ushigome**[2]
Lukas Franciszkiewicz[2] **Deepak Chandra**[3] **Ivan Poupyrev**[3] **Ramesh Raskar**[1]

[1]MIT Media Lab
munehiko@acm.org, {rohan, olwal, raskar}@media.mit.edu

[2]Takram London
{ushi, lukas}@takram.com

[3]Google ATAP
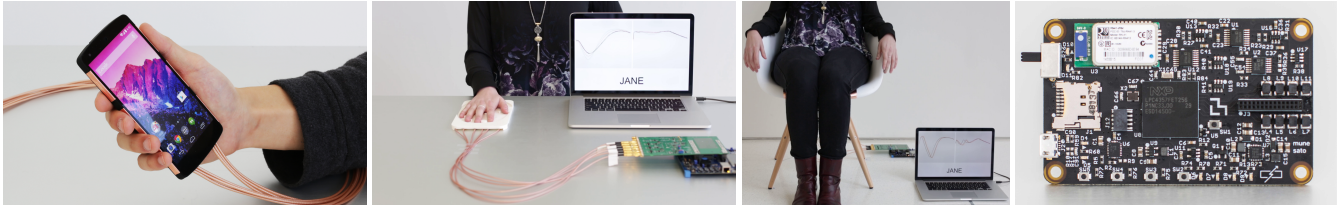{dchandra, ipoupyrev} @google.com

Figure 1. *Zensei* embeds implicit and uninterrupted user identification in mobile devices, furniture or the environment. Our custom, wide-spectrum multi-electrode sensing hardware allows high-speed wireless data collection of the electrical characteristics of users. A longitudinal 22-day experiment with 46 subjects experiment shows promising classification accuracy and low false acceptance rate. The miniaturized wireless *Zensei* sensor board (right) has a microprocessor, power management circuit, analog sensing circuit, and Bluetooth module, and is powered by a lithium polymer battery.

ABSTRACT

Interactions and connectivity is increasingly expanding to shared objects and environments, such as furniture, vehicles, lighting, and entertainment systems. For transparent personalization in such contexts, we see an opportunity for embedded recognition, to complement traditional, explicit authentication.

We introduce Zensei, an implicit sensing system that leverages bio-sensing, signal processing and machine learning to classify uninstrumented users by their body's electrical properties. Zensei could allow many objects to recognize users. E.g., phones that unlock when held, cars that automatically adjust mirrors and seats, or power tools that restore user settings.

We introduce wide-spectrum bioimpedance hardware that measures both amplitude and phase. It extends previous approaches through multi-electrode sensing and high-speed wireless data collection for embedded devices. We implement the sensing in devices and furniture, where unique electrode configurations generate characteristic profiles based on user's unique electrical properties. Finally, we discuss results from a comprehensive, longitudinal 22-day data collection experiment with 46 subjects. Our analysis shows promising classification accuracy and low false acceptance rate.

[*]Secondary affiliation: The University of Tokyo (Tokyo, Japan)

[†]Secondary affiliations: KTH – Royal Institute of Technology (Stockholm, Sweden); Google Inc. (Mountain View, CA, USA)

ACM Classification Keywords

H.5.2. Information interfaces and presentation: User Interfaces - Graphical user interfaces; Input devices & strategies.

Author Keywords

Implicit sensing; User recognition; Ubiquitous computing, Electrical sensing; Embedded devices; Bio-sensing

INTRODUCTION

People are interacting with more and more smart devices such as mobile phones, tablets, laptops, and public displays. Now, interactions are also expanding to furniture, lighting, home automation devices, personal and transportation vehicles, and other everyday objects.

As objects around us are becoming Internet-connected, shared, and *smart*, it will be increasingly important to personalize the experience during interaction. When user interactions are frequent, recognition procedures should be as transparent as possible, to minimize interruptions such as prompts for passwords, personal identification numbers (PIN), or biometric verifications (e.g., fingerprints or iris).

Such procedures might also create unnecessary complexity for tasks with limited privacy implications, such as automatically adjusting user car seat preferences. More relaxed recognition may be useful in such scenarios due to the potential for transparent and uninterrupted interaction. We are also seeing increasing use of multi-factor authentication, where users are allowed access through, e.g., the use of a secret (e.g., password, PIN) and a physical item in their possession (e.g., mobile phone, bank card, security key) or by proximity. Such mechanisms improve robustness, but can also introduce even more friction.

User identification today is tedious, but necessary, especially in scenarios in which users share a single device but have

their own preferred settings or interaction styles. This includes shared TVs, video games, cars, phones, computers and tablets.

We envision that implicit user identification and automated customization will be of significant importance now that everyday objects are being augmented with computational power and network connectivity.

We thus see an opportunity for bio-based recognition techniques to use implicit and transparent sensing to minimize the need for explicit authentication by the user. We also envision that bio-based recognition could complement existing techniques by providing the benefits of multi-factor authentication without explicit interaction burden on the user.

Zensei enables physical objects to identify users by sensing the body's electrical properties and touch behavior through electrical frequency response sensing. It allows almost any object to be capable of user recognition. For example, a phone that unlocks as it is picked up, a car that adjusts the mirrors and seat based on the driver, or a shared tablet that activates parental mode when a child holds it (Figure 1).

Zensei is a new approach of implicitly recognizing users by their body's electrical frequency response properties, with the following contributions:

Contributions
1. Custom bioimpedance hardware that measures both amplitude and phase and extends previous approaches through a wide range of frequencies over multiple electrode combinations, while enabling high-speed wireless data collection in a compact and embedded form factor.

2. A set of form factors (hand pad, chair, and smartphone), where unique electrode configurations generate characteristic profiles based on a user's unique electrical properties.

3. A comprehensive longitudinal data collection experiment with 46 subjects over 22 days. Our analysis shows promising classification accuracy and a low false acceptance rate.

RELATED WORK AND APPROACHES
User identification and authentication technologies have a long history including various proposed approaches. Here, we specifically discuss biometric techniques, and how Zensei builds on prior art.

Capacitive and Impedance Sensing of the Body for HCI and Security Applications
Capacitive and impedance sensing of a user's body has been widely employed in HCI. Arrays of capacitive sensors covering surfaces have been used to enable touch and gesture sensing. However, this work mostly focuses on flat or curved planes due to relatively complex configurations and manufacturing processes [36, 29, 45, 46, 48, 42, 38, 32]. These capacitive sensing techniques are generally measuring the amount of electrode contact, such as surface area, insulation thickness, and touch pressure through fingertip deformation. *Zensei* extends these architectures by measuring the impedance through the body tissue through the capture of electrical response between pairs of electrodes. *Zensei* leverages this capability to identify who is touching the object because of the differences in body tissue composition (Figure 1).

DiamondTouch [14] uses capacitive sensing to measure the coupling of a user's body between a large sensing touchscreen and a receiver, and disambiguates users based on the electrodes that they are touching or sitting on. SkinTrack [52] continuously tracks skin touch with a finger-worn transmitter and a wristband device.

Human tissue bioimpedance measurement techniques [31] have been shown to be both versatile and widely applicable for advanced sensing. Applications include blood coagulation monitoring [30], breast cancer detection [26], human body fluid composition measurement [17], and commercial health products such as body fat scales. More complex and controlled scanning configurations have enabled techniques such as electrical impedance tomography (EIT) [9, 4], to enable imaging inside the body with an array of sensing electrodes in a cross-section. These approaches served as inspiration for *Zensei*, where we use a small number of sensors to explore tomographic scanning for user-specific body characteristics.

Intra-body communication was proposed by Zimmerman et al. as a Personal Area Network (PAN) [55, 54]. PAN, or Body Area Network (BAN), is a method for communication between devices on or near users' bodies. PAN uses capacitive coupling of pico-amp currents that are transmitted through the body with data rates of 300 [55], 2400 [54] or 9600 bps [34]. Body-Coupled Communications (BCC) [3] enabled even higher data transfer speeds (10 Mb/s). These techniques mainly focus on using the body as a data communication medium and to ensure that two devices are on the same body, although Post et al. also proposed transmitting power over a PAN [34]. EnhancedTouch [44] senses human-to-human touch with wrist-worn devices. *Zensei* focuses on using the human body to characterize the user, rather than as a digital data communication path.

Tomo [51] applied Electrical Impedance Tomography (EIT) to a wristband-shaped gesture recognition system. It measures interior impedance geometry with eight electrodes in a wristband. The system recognizes gross hand and thumb-to-finger pinch gestures. Biometric Touch Sensing combines a wristband bioimpedance sensor and a touch-screen computer for an integrated authentication technique [25]. *Zensei* explores how similar hardware can be embedded in devices and furniture to allow uninstrumented users to be recognized.

Swept Frequency Capacitive Sensing (SFCS) was shown to capture the body's capacitance using a single sensing electrode to detect gestures on various everyday objects [39], and to differentiate between touch-screen users (with no simultaneous multi-user touches) [21]. In the SFCS configurations, whole-body capacitance is measured with a common ground connection [39, 21].

Biometrics: Conventional and Bioimpedance-based
Passwords are the most common authentication method, but have major disadvantages. They need to be remembered, can be observed, and tend to be reused [15, 22]. They are especially problematic due to the risk of theft and access [16].

Biometric approaches use physiological and behavioral characteristics for recognition. Commonly proposed biometric authentication techniques include sensing of the iris, face, gait,

superficial vein structure, fingerprint, ear shape, hand geometry, retinal pattern, palm print, bone conduction through the skull, voice, written signature, and DNA [27, 19, 5, 47, 24, 20, 40]. Yampolskiy and Govindaraju describe behavioral biometrics in a comprehensive survey [50], whereas Cornelius and Gutierrez focus on mobile contexts in their survey [11].

One of the most popular biometric techniques is fingerprint recognition, which is widely used by border control agents, laptop computers, and more recently in smartphones such as the Apple iPhone's TouchID [1] and the Sony Xperia Z5 [43]. TouchID and Xperia Z5 combine a home button and a fingerprint scanner to provide an integrated user experience with a one-step interaction, while reducing the burden of aligning a particular fingertip. Similarly, FiberIO [23] captures fingerprints on rear-projected touch screens. It authenticates users during interaction using a fiber optic plate and a high-resolution camera. Behavioral approaches analyze, e.g., fingertip locations on multi-touch displays [6], how displays are touched [53], how users type on touch-screen keyboards [33], and GUI element targeting behavior on a touch-screen [8].

Some recent consumer products, including Jawbone's UP3 [28] activity tracker and Samsung's Simband [37], measure bodily functions, such as blood flow, heart rate, respiration rate, hydration levels and galvanic skin response (GSR), but currently do not use this data for user recognition.

Rasmussen et. al. [35] propose to complement PINs through the use of the frequency domain of the temporal response from a square-pulse between two brass electrodes that the user holds. They discuss an experiment that was conducted with laboratory bench-top instruments (a wave generator and oscilloscope) with ten subjects.

Cornelius and colleagues measure bioimpedance around users' wrists for security applications [12, 13], and report detailed evaluations of electrode arrangement, permanence, and longitudinal effects with special wristband-shaped sensors [10]. They also demonstrate passive user recognition [12] using a custom Shimmer [41] bracelet with an array of electrodes. Eight participants wore the device for a day, and additional data was collected from three of those participants after 140 days, with consistent results.

Zensei builds on this work by exploring a broader range of devices and form factors, and daily data collection over several weeks from a larger subject pool. We also introduce custom sensor hardware to enable high-speed wireless data collection for embedded devices.

ZENSEI: WIDE-SPECTRUM BIOIMPEDANCE SENSING FOR OBJECT AUGMENTATION

We advocate an approach to capture a user's body's electrical characteristics by implementing sensors into the physical objects around us. Our approach shares some similarity with SFCS [39, 21], however, we measure both the amplitude and phase components of the electrical frequency response and do so among all combinations of up to eight embedded electrodes. Medical studies show correlations between phase ad body properties, such as Body Mass Index (BMI), sex, and age [7]. While SFCS uses a single electrode and measures
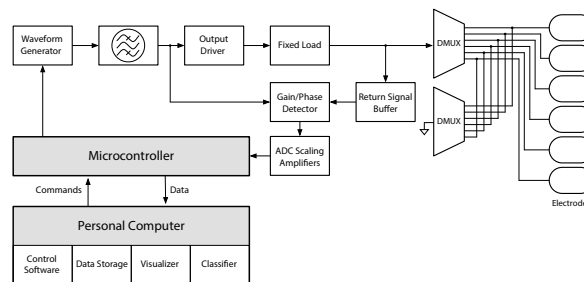

Figure 2. *Zensei* **system block diagram. PC and sensor board with microcontroller and analog sensing circuits. The electrical properties between two sensor electrodes are captured using a gain and phase detector IC.**

the impedance between the electrode and the ground (earth), *Zensei* measures the impedance between multiple pairs of electrodes with shielded cables (Figure 2 and 3).

In our approach, we designed and developed prototypes to demonstrate three different form factors that evaluate and exhibit *Zensei*'s versatility. These include static sensing with relatively stable and controlled user touch behavior (*Hand Pad*), semi-static sensing with variable user touch behavior but stable skin contact (*Smartphone*), and variable sensing with variable touch behavior due to user posture and changes in clothing (*Chair*). The chosen form factors are also representative of a range of use cases where this technology can have an impact, from mobile devices to furniture.

Hand Pad. Six electrodes are arranged on a 3D-printed mold, shaped after a generic right hand. The disc-shaped electrodes (8 mm diameter) are placed at the five fingertips and the palm near the base of the thumb (abductor pollicis brevis), as shown in Figure 4, left. We are using silver/silver-chloride (Ag/AgCl) electrodes, originally designed for electroencephalography (EEG) and electrocardiography (ECG), which are safe for use in direct contact with human skin.

Chair. Six electrodes are arranged on a chair surface where the hip, thigh, back, and arm can comfortably make contact with the molded single-piece plastic shell. Electrodes are made of thin copper tape, and are covered with thin plastic adhesive tape to properly condition the experiment to prevent direct skin contact. The dimensions of each electrode are approximately 50 mm × 200 mm (Figure 4, center).

Smartphone. Six electrodes are arranged on the two sides of a replica LG Nexus 5 smartphone (three on the left edge and
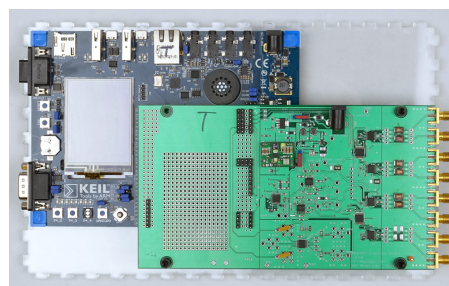

Figure 3. *Zensei* **prototype sensor boards used for data collection and evaluation. Sensor boards consist of an ARM Cortex M4 evaluation board and a custom analog sensing board.**

Figure 4. The three prototype configurations: *Hand Pad*, *Chair*, **and** *Smartphone*, **and their electrode arrangements. Colors indicate the electrode connection position on the custom sensor board.**

three on the right). The electrodes are made of thin stainless steel tape and are directly exposed to user touch. The dimensions of the electrodes are 30 mm × 5 mm (Figure 1, top left, and Figure 4, right).

Sensing System Overview

Zensei was implemented with custom-designed sensor boards; (1) a prototype board stacked on top of a microprocessor evaluation board (Figure 3), and (2) a fully integrated, wireless, and embeddable sensor board (Figure 1 right). The first board is used for our evaluation and analysis.

The high-level system diagram for *Zensei* is shown in Figure 2. The sensing procedure is as follows. The signal generators create sine waves at a range of programmable frequencies. The signal is then amplified and outputs at a select electrode pair. A part of the user's body touches the electrodes, and the return signal's amplitude and phase component are captured with the Analog-to-Digital converter (ADC) port of the microprocessor and RF gain and phase detector IC. Our current sensor board hardware supports up to eight electrodes, however, we only used six electrodes with the evaluation in this paper to match and compare against our first form-factor (i.e., five fingertips and palm). The captured amplitude and phase data are transferred to a PC to be processed by a machine learning classifier.

Implementation

General Hardware Design

Our implementation uses an NXP LPC4357 (ARM Cortex-M4 204MHz) microprocessor evaluation board (KEIL MCB4357) along with a custom analog sensing extension board. We employ Analog Devices' AD5932 wave generator IC to create a sinusoidal wave, and the AD8302 RF Gain and Phase Detector for impedance measurement. In our evaluation with the first-generation board, we used a passive envelope detector circuit for amplitude measurement, and AD8302 for absolute phase measurement. The sensing signal is ±3.3*V*.

The electrode connections are controlled by analog demultiplexer (DMUX) circuits on the sensor board, and the sensing electrode and ground electrode are switched among the multiple electrodes after each set of frequency sweeps is completed. For six electrodes, there are 30 electrode pairs ($n \times (n-1)$). The ground is rotated in sequence among the six electrodes by measuring in pairs with the remaining five. Figure 5 shows how a particular electrode input index corresponds with the same color graph. E.g., the red electrode is the sixth electrode input on the board and goes to the palm, left arm, and right
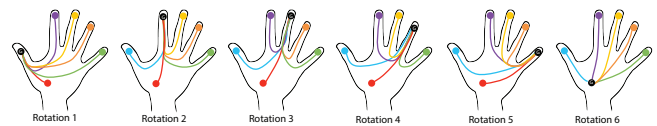

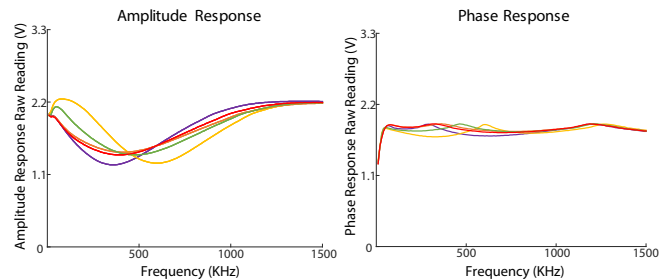**Figure 5. Electrode demultiplexing and ground electrode rotation.**

Figure 6. Amplitude and phase curves. Colors correspond to the electrodes shown in Figure 4 for a given single ground electrode. The differences of each curve represent the slightly different electrical frequency properties between pairs of electrodes. Raw data demonstrations from evaluation are shown in the Appendix.

bottom electrode on the hand pad, chair, and smartphone rigs, respectively.

We chose electrode materials that are suitable for each application and form-factor. We chose medically-safe materials (silver/silver-chloride and stainless steel) for electrodes that touch the skin directly (*Hand Pad* and *Smartphone*). For furniture, we used thin, adhesive copper tape, insulated with plastic tape, which is easier to cut and apply to non-planar surfaces (*Chair*). The AC coupling that we use in this system is extremely low. Direct coupling to an AC signal as such is considered absolutely safe from a clinical perspective and a similar technique is commonly used in consumer body-fat scales and medical bioimpedance tomography units.

The amplitude and phase component of frequency response reading outputs are digitized by 10-bit ADC ports on the microcontroller. The actual captured impedance and phase curves for a given rotation position are shown in Figure 6 where the color of the curves indicates which excitation electrode was used. The reading is the raw voltage at the ADC. The amplitude response of the user's body is measured via a voltage divider with a fixed load on the circuit. The phase difference caused by the user's body is measured as the VPHS output of AD8302 IC. Our current implementation uses RG-316 coaxial cables and SMA connectors (50Ω) to connect the sensing circuit and electrodes to ensure the reliable signal shielding. In our future implementations, we plan to use thinner wires and smaller connectors to enable more compact form factors.

Real-Time Visualization and Data-Collection Software

Data from the hardware implementation is processed, and interpreted by custom visualization software (both in Java and C++). This software allows the frequency sweep parameters and paired-electrode configuration to be changed. Our implementation also includes real-time machine learning, classification, and data-storage capabilities. The real-time classification speed is most limited by the number and value of frequencies being swept and the classification time by the model. In our

case the sweep time for all combinations of electrodes, including three periods of each frequency for the signal to stabilize, was approximately 140ms. Our prototype system adds 300ms overhead for data processing, hand-off, and classification. We plan to optimize the system in future implementations by using a smaller number of frequencies and processing more data on the device to minimize data transmission delay.

Changes Made for Miniaturized Wireless Boards

We also developed a wireless board (50.8 mm × 83.6 mm, 20 g) with an improved circuit design that uses dual wave generator ICs to create two separate wave outputs with a programmable phase difference (Figure 1, right). This enables determination of the sign of the phase shift with an AD8302 RF gain and phase detector that cannot determine the sign of the phase by default. The wireless PCB also allows enables optional ungrounded sensing.

EVALUATION
Data Collection Procedure

We collected data from an initial group of 74 subjects to evaluate the identification performance of *Zensei* in three form-factors (*Hand Pad*, *Chair*, and *Smartphone*) over a 30-day period (data collection on 22 workdays)[1]. The experiment was designed to introduce a realistic amount of inter-subject physiological diversity, time-based physiological changes, and subject behavior variability. We report on the Classification Accuracy (CA), False Acceptance Rate (FAR), and False Rejection Rate (FRR) of the configurations.

Participants were all working professionals outside of academia and recruited voluntarily from an external subject pool through a user testing agency. Each subject was assigned an anonymous username and asked to provide basic biographical information. Subjects ranged in height (1.63–1.96 m, mean=1.76±0.10 m, weight (56.7–133.8 kg, mean=82.2±18.8 kg), BMI (18.0–46.7, mean=26.4±5.4), skin type (dry–oily), age (20–56 years, mean=33.23±8.87 years), ethnicity, and gender (26% female, 74% male).

To introduce time-based physiological changes, subjects were asked to provide five data samples per session in two sessions per day, once in the morning and once in the afternoon, during their workdays. This timing allowed for realistic changes in clothing, skin condition, and body composition. An individual subject could have provided a maximum of 660 samples for the duration of the experiment. (3 *prototype setups* × 5 *samples* × 2 *sessions* × 22 *workdays* = 660 *samples*.)

Twelve subjects provided data in at least one session per day for all 22 days. This dataset, *Dataset A*, was used for the hold-one-day-out and buffered training evaluations, as well as the electrode configuration and subject confusion analyses. Forty-six subjects participated in two sessions per day for at least 13 days (not necessarily consecutive). This dataset, *Dataset B*, was used for the subject pool size evaluation. The remaining sixteen subjects were not included in the analysis since they did not fit either of the above criteria.

Subjects were instructed to follow a short procedure for each sample collection session:

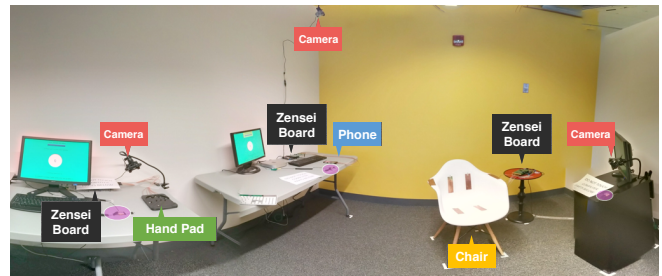[1]This study was approved by the IRB of the authors' institution.

Figure 7. Experimental setup. Anti-static wrist straps (pink) are used to discharge static before starting data collection. Web cameras, used for data verification, are shown in red.

1. Place right hand on Hand Pad. Lift up hand. (Five times)

2. Pick up mock-up smartphone to read the screen, as you would normally do. Put down phone on table. (Five times)

3. Sit down in the chair. Get up and off the chair. (Five times)

This procedure was designed to add realistic subject behavior and interaction variability into the collected data.

The hardware was applied an excitation signal at a frequency sweep from 1 KHz to 1.5 MHz in 150 linear steps. Data was collected on three personal computers and stored for subsequent data processing. The first four days of results of the hand pad were not used in the analysis because its circuit board had malfunctioned and had to be switched out.

A given data sample is composed of 60 vectors of 150 points of data (30 vectors for the amplitude response and 30 vectors for the phase response of 150 different frequencies) compiled and labeled by username and timestamp for easy segmentation.

We created one data collection kiosk for each configuration (a computer, monitor, keyboard, sensor board, and one of either the hand pad, chair, or smartphone), for a total of three kiosks as shown in Figure 7. The kiosks were set up in an air conditioned office building room near where most subjects worked to encourage daily morning and afternoon participation. The entire data collection was done in the same room. The computers and sensor boards were grounded. Background over-the-air EM radiation is assumed to have significantly lower power than our system signals, and it did indeed not introduce problems.

Web cameras took photos when samples were collected to verify full electrode contact for the hand pad, holding as if reading with the phone, and sitting back into the chair with arms on the armrests. Samples that, upon photo inspection, did not adhere to the above (no electrode contact) were removed from the datasets. In total, 447 samples were removed (1.3% of the entire dataset).

To prepare the data for classification, the 60 vectors were first smoothed using a moving average filter (n=5). It was empirically determined (from a separate training and validation set) that good performance was achieved by feeding this smoothed data into an SVM classifier with Polynomial Kernel (E=1.0, C=1.0). We used the SMO implementation in the WEKA Toolkit [49] to train our SVM classifier. The classifier was
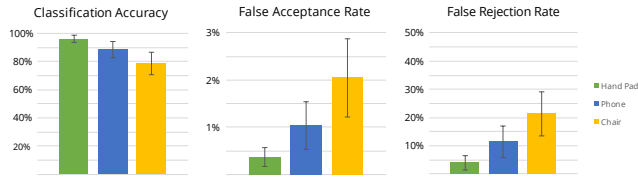
Figure 8. Hold-One-Day-Out Classification Accuracy (CA), False Acceptance Rate (FAR), and False Rejection Rate (FRR) for *Dataset A*. Error bars represent standard deviation (SD).

designed to identify the correct participant from separated participant training and test sets. We include the FAR and FRR to better understand error rates.

User Classification Analysis

Hold-One-Day-Out Evaluation

It is well known that an individual's electrical properties can change over time, for example, due to changes in levels of environmental humidity or user tissue changes (e.g. sweat, fat, and hydration levels) [17]. As a preliminary evaluation of classification accuracy over the full time-period, we performed a hold-one-day-out validation on *Dataset A* by training our classifier on 21 days of data and testing on the remaining day for every combination of days and averaging all resulting combinations. As shown in Figure 8, the more constrained arrangements (hand pad) tend to outperform those with more user behavior variability. Additionally, the chair showed lower performance likely because of the strong influence of the subject's clothing in the collected signal. Overall, the high accuracy and low FAR are promising considering the relatively challenging long-term and variable scenarios in which the data was collected. However, the higher FRR could restrict some application scenarios.

Buffered Training Evaluation

Next, to evaluate the number of days of variability necessary to maximize classification accuracy, we explored varying numbers of training days. To do this, we trained our classifier with samples from days $[0 \rightarrow t]$ days where t is shown on the x-axis of Figure 9, 10, and 11. The training data was then tested on each individual subsequent day (days $[(t+1) \rightarrow 22]$) and averaged together. This would be most applicable to keeping a running buffer of training data on a personal device. In this case, our results suggest that the training buffer becomes relatively stable after about nine days of collected training data. The FAR and FRR for the *Hand Pad* configuration reduce over accumulating days of training. This trend indicates that the system can build a stronger classifier with varied training data collected over a long period. The FAR and FRR for the *Chair* do not drop as the *Hand Pad* does. This could be because the subjects wear different clothing every day, with and without sleeves, which results in more signal variability. The inconsistencies for the *Phone* were likely observed because of variability of grasping style within a single subject. We explore specific reasons for such confusions in the discussion.

Subject Pool Size Evaluation

Finally, *Dataset B* was sectioned off into subsets of subjects to create pools of 5, 15, 25, and 46 subjects. These pools were created by taking the first *N* subjects from the pool (chronologically according to first participation date) from the original
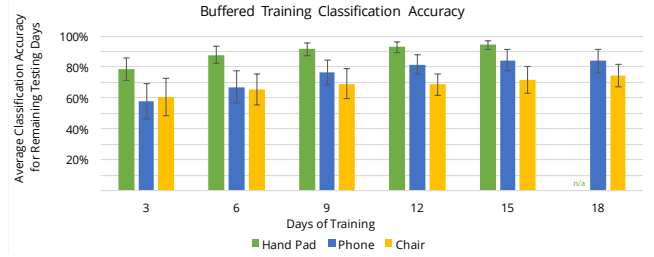

Figure 9. Average buffered training classification accuracy on subsequent days for 12 subjects (*Dataset A*). Error bars (SD) indicate performance of multiple combinations of data for a given average. Hand Pad 18-day data excluded due to initial technical issue.
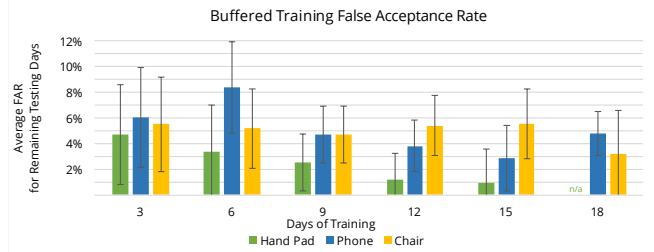

Figure 10. Buffered training FAR on subsequent days for 12 subjects (*Dataset A*). Error bars (SD) indicate performance of multiple combinations of data for a given average. Hand Pad 18-day data excluded due to initial technical issue.

46-subject dataset, where *N* appears on the x-axis of Figure 12, 13, and 14. Then, the first 13 days of complete participation (i.e., >=2 sessions of captured data) for each subject were split into every combination of 12 training days and one testing day for evaluation. The resulting 13 combinations for each subject pool size were then averaged, as shown in Figure 12.

Among the three form-factors, the *Chair* condition shows the least favorable results, especially for five participants (Figure 12, 13, and 14). This is mainly because of the low amount of variation of the captured signals due to the capacitively-coupled garments. The classification performance is improved by accumulating more days of training (Figure 9, 10, and 11). We expect that the performance will be more robust and consistent in more specific scenarios, such as commercial drivers with uniforms. *Zensei* could also benefit such scenarios by transparently complementing physical tokens, such as ID badges or keys, which are vulnerable to theft and forgery.
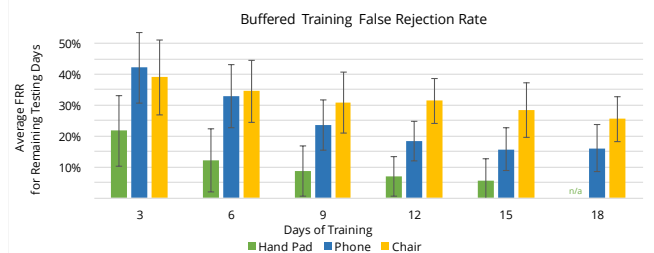

Figure 11. Buffered training FRR on subsequent days for 12 subjects (*Dataset A*). Error bars (SD) indicate performance of multiple combinations of data for a given average. Hand Pad 18-day data excluded due to initial technical issue.
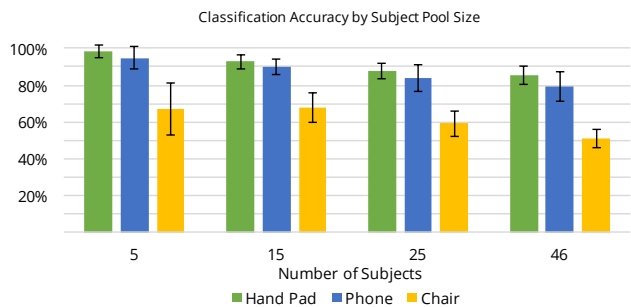
Classification Accuracy by Subject Pool Size

Figure 12. Classification accuracy on increasingly larger subject pool sizes (*Dataset B*). Error bars represent SD.

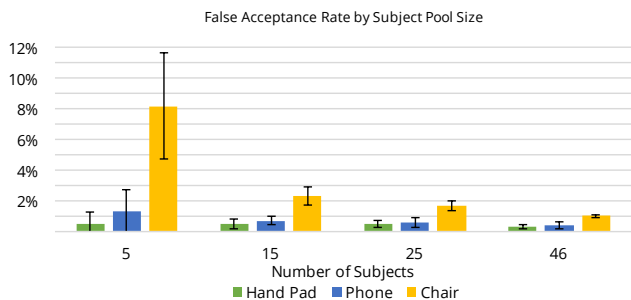False Acceptance Rate by Subject Pool Size

Figure 13. FAR on increasingly larger subject pool sizes (*Dataset B*). The Chair condition results in relatively high FAR for five subjects, but improves drastically for 15 and higher. Error bars (SD) indicate performance of multiple combinations of data for a given average.

Electrode Configuration and Subject Confusion Analysis

In order to better understand the reason behind the subject classification accuracies observed, the data from each rig was further evaluated to firstly peer deeper into certain electrode combinations and secondly determine the most likely causes for misclassifications between subjects. In the former case, the data was divided to understand what number of electrodes and specific electrode combinations achieved the highest classification accuracies on their own. In the latter case, we used patterns in resulting confusion matrix data, recorded behavioral interaction photo data, and pre-collected subject anatomical data to determine the most probable cause for consistent confusions between subjects.

Electrode Configuration Performance

As part of a preliminary evaluation of electrode influence on classification accuracy, we first iteratively trained and tested all possible combinations of all numbers of electrodes (i.e., two, three, four, and five electrode groups) using the previously described classification technique. In this evaluation, the first 21 days were trained on and then tested against the final day for all electrode combinations in a given electrode group. The evaluation used the final day of *Dataset A*'s subject data to reduce computational load, given the large number of evaluations needed if all combinations on all 22 days were used.

We observe that, in general, a higher number of electrodes results in higher classification accuracy as shown in Figure 15. We can attribute this increased accuracy simply to a larger amount of anatomical and behavioral data being sensed be-
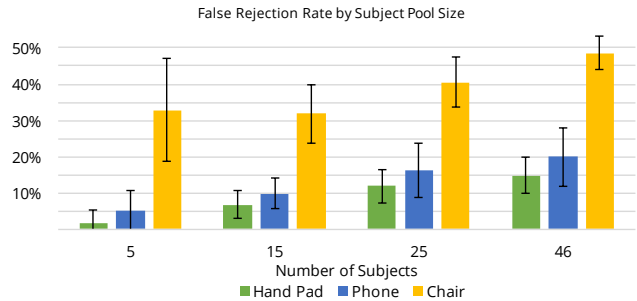
False Rejection Rate by Subject Pool Size

Figure 14. False Rejection Rate on increasingly larger subject pool sizes (*Dataset B*). Error bars represent SD.

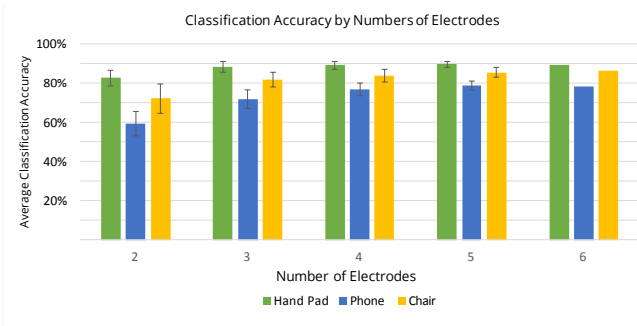Classification Accuracy by Numbers of Electrodes

Figure 15. Performance for all combinations of a given number of electrodes using *Dataset A* on the last day of testing only. Specifically, the model was trained using data from all days except the final day, and then evaluated on the final day. Error bars represent SD. SD excluded for the six electrode group due to only one possible electrode combination.

cause of a great surface area being covered by the sensing electrodes. However, this trend in accuracy begins to level off around four electrodes, demonstrating that a lesser number of electrodes may suffice for some implementations.

Next, the specific electrode combinations were evaluated against each other and the highest classification accuracy combinations for each electrode group (i.e two, three, four, and five electrode groups) were identified. As shown in Figure 16, the highest accuracy electrode combination for the two-electrode group also appeared in all other top performing combinations for the remaining groups.

For the Hand Pad, electrodes one and four, the index and pinky electrodes, were most significant in their impact towards recognition, followed closely by the palm. For the index electrode, we note in our captured image data that many users begin to align their hand to the electrodes using the index finger as a starting point. This ensures more reliable alignment and skin contact at this electrode which may point to why it is an important factor in classification. In contrast, the middle and ring finger are slightly more difficult to manipulate and thus do not show reliable alignment. Additionally, we observe that in our testing arrangement, the pinky electrode may have been slightly too far for some subjects and thus served as an important identifier of subject hand size. However, we do not see correlations between average human finger length variation and accuracy for any of the other electrodes which were consistently touched. Finally, we note that the electrodes in group three are relatively evenly spread out with maximum
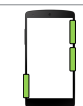
Figure 16. Highest performing electrode combination for each electrode combination group (two, three, four, and five electrode groups) on all three rigs by training on all but the final day of *Dataset A*, and classifying on the remaining day. Classification Accuracy (CA), False Acceptance Rate (FAR), and False Rejection Rate (FRR) for each electrode group.

distance from each other on the hand. This may relate to the existence of more identifiable anatomical information between points that are farther apart. All these factors indicate that the classification accuracy in the Hand Pad is both a combination of electrode alignment and the electrical properties of the hand.

The phone rig's strongest electrodes were the right-top and right-center electrodes. One reason for this is the variety of different grasps that the subjects used when grabbing the phone. Subjects with smaller hands or those who were naturally left-handed could not reach the right-top electrode. We observed that grasping style significantly impacted contact with the right-center electrode as well, depending on thumb wrapping behavior (e.g., placing the thumb on the screen or on the side of the device). However, despite these behavioral differences, subjects with similar grasps could still be differentiated.

Finally, the chair rig's top performing electrodes were the bottom-left and right-arm electrodes. The back electrodes seem to switch in priority as well between the four-electrode and five-electrode group, demonstrating to us that these electrodes might not be as reliable because of different sitting styles and additional layers worn by subjects due to winter weather. The bottom and arm electrodes, in contrast, provided more reliable contact in most cases and had thinner clothing layers and less day-to-day variability. This is likely because clothing on these areas is less variable and user weight and arm resting style play in as a factor on these electrodes.

DISCUSSION

Our results illustrate the potential for implementing *Zensei* as a technique for implicit user sensing in ubiquitous computing scenarios, without the need for user instrumentation. The data collection and analysis show that the important factors that influence *Zensei's* performance include the amount of training data under different conditions, contact and alignment with electrodes, subject pool size, and electrode configuration.

Evaluations (Figure 9, 10, and 11) indicate that *Zensei* can benefit from a large amount of up-front training to define user behavior. One of the most important advantages of *Zensei* is that we can continuously sense and collect training data as the user interacts with *Zensei*-instrumented devices and environments. Depending on the application, *Zensei* could collect electrical property data in the background when the device is used with traditional identification. Then, after sufficient data is collected for reliable identification (as evaluated in Figure 9), customization features could be suggested to the user.

Another challenge is how to best ensure consistent measurements. Our results show that performance is affected as form factors allow increasing variation in alignment, contact and material between body and electrodes. E.g., if a particular user tends to change their smartphone grasping style dramatically, it will be important to be able to correct for rotated alignments, or sufficiently learn variable grasping behavior before automatically customizing their experience. A thorough training process will help improve classifier robustness.

The hand pad shows how consistent measurements through mechanical alignment improves performance. This demonstrated that even with consistent contact and surface area, we could still distinguish among small groups of individuals. This approach is directly applicable to devices and tools with clearly defined grips, such as power tools, garden tools, and kitchen appliances (e.g., handheld mixers). For general-purpose electronics, however, restricting specific grasping limits the industrial design options and the seamless integration of *Zensei* into everyday devices. We are, however, interested in exploring other strategies to ensure consistent measurements for such use cases. This could include external sensors (e.g., pressure, proximity, switches, and cameras) to automatically detect appropriate alignment and contact, and then label samples accordingly. Other strategies would include detecting user activities where physical alignment is mechanically constrained or well understood, such as using a keyboard on a smartphone.

From a physiological standpoint, identification using the body's electrical properties may not work as well for users who experience large fluctuations in biological properties throughout the day (e.g., sweating profusely) or who live in highly variable weather and humidity conditions. To address this, more samples will need to be taken throughout in a variety of conditions. Additionally, devices with variable electrode-skin touching behavior (e.g., smartphones) need to cope with both physiological and behavioral change throughout the day. E.g., smartphone grasping styles while walking may dramatically differ from grasping at night, while reading in bed.

Our quantitative analysis of classification accuracies, false acceptance rates, and false rejection rates suggests that *Zensei* currently is primarily suitable for smaller groups of users, such as a household, work team, members in a carpool, or in social groups like for multi-player gaming. The current classification method is also limited in that it requires the model to be retrained as new users are added.

Furthermore, the current user differentiation accuracy is not sufficient for critical security applications. For standalone use, *Zensei* is, instead, more suited for lightweight and unobtrusive customization of applications. We do, however, see potential in combining *Zensei* with other authentication technologies to enable multi-factor authentication without added effort for the user. The hand pad's controlled placement, for example, makes it particularly suitable in combination with optical sensing (e.g., finger print, hand geometry, palm print and vein structure), where *Zensei's* bioimpedance sensing is less vulnerable to theft and can add robustness.

In environments where a limited number of simultaneous users are expected, we envision that *Zensei*-instrumented devices could be combined with wireless scanning of mobile devices. This would help assess which users are present, and thus simplify disambiguation and increase classification confidence.

Our implementation is based on commercially available waveform generator ICs and gain/phase detector ICs with limited phase measurement range, resolution and accuracy. This makes our approach readily accessible to other researchers for replication, validation and enhancements. However, that classification performance could improve with a complete implementation, through ground-up engineering, IC design and manufacturing. Thus, we hope that future work will further the understanding of the comparative contribution of different components' role for bioimpedance in prediction accuracy for HCI applications.

APPLICATIONS: IMPLICIT USER RECOGNITION FOR DEVICES AND ENVIRONMENTS

Based on our results, we have identified a set of representative scenarios, that we believe illustrate the unique advantages of *Zensei* to implicitly enable customization through instrumented devices and furniture.

Hand-based User Recognition for the Internet of Things: Grasping and Touching

Zensei could be used as a touch-based identification system to customize experience with an informational device or home appliance. When an individual wants to be identified by the system, they just need to place their hand on the handle. *Zensei* scans the electrical properties of the user's hand and the kiosk can then recognize and present useful information to the user as shown in Figure 1. This identification technique can be specifically useful for casual customization. For example, refrigerators at home may in the future have a *Zensei*-embedded control panel, and show how often you are opening the refrigerator and give health advice. In other scenarios, remote controls could be aware of who is holding them and display suggested movie titles based on user preference and history. The recognition accuracy could be improved by using other sources to understand who is present, e.g., based on expected users in a house or wireless scanning of mobile devices.

As *Zensei* uses multiple embedded electrodes for sensing, users could grab a *Zensei*-equipped doorknob in a certain way when opening a door. Interaction with a doorknob is a unique opportunity to capture and customize a user's next intended interaction in the room they are entering. By sensing in this

Figure 17. *Zensei* **enables whole-body user recognition through instrumented furniture.**

way, we could create powerful "user-specific commands" that are made from a combination of physiological and behavioral features. This could allow users to provide different instructions to their "connected home" from throughout the building, without needing a special console. The home could then understand and interpret these commands from the context of the user who is instructing them. For example, a grasp gesture on the door while entering the home could initiate preferred temperature and lighting settings. Similarly, a smart coffee machine could customize a cup of coffee according to who has entered the kitchen and instructed the start of breakfast through the doorknob.

Whole-Body User Recognition: Ubiquitous Computing, Vehicles and Furniture

Interactions between humans and the objects around them is not limited to the hands. The trunk, limbs, feet, and other body parts are also used for everyday interactions in our living environment. Because *Zensei* uses an AC Signal, it does not require direct skin contact. This allows *Zensei* to be used in a variety of scenarios in which clothing or object material may get in the way of other methods.

Zensei could enable connected furniture to customize the user experience by remembering user presets user, as shown in Figure 17. A car seat could sense who is sitting in it, and adjust seat height, mirror angles, and radio channel. Furthermore, it could prevent a child from driving the car. We also envision a co-working electrical desk that knows who is working at it and automatically adjusts its height. It would also be possible to augment shared home training equipment that adjusts the weights to the family member that sits on a bench, and keeps track of individual repetition counts.

These scenarios can be enabled without user instrumentation, through the use of embedded sensing electronics. All instrumentation is done on the object side and is invisible from the outside. This gives furniture and interior designers creative freedom while also keeping the burden on users to a minimum.

User Recognition for Portable Devices: Mobile Phones, Remotes, and Electrical Tools

By augmenting portable devices, we can provide transparent access to information through our user identification method (see Figure 1). Because *Zensei* can be adapted to almost any shape, it can be built into the housing of everyday handheld devices such as smartphones, tablets, and TV remotes, as well as, electrical tools.

We demonstrated a smartphone with six embedded electrodes. *Zensei* learns both the physiological properties of the user and the ways in which the user typically holds the smartphone in order to recognize them later. In situations where a phone

or tablet may be on a table in a shared environment with a small and typically known group of people, such as an office or at home, the implicit recognition using *Zensei*, could allow unlocking certain features on the device, similarly to how one may access the camera and notifications today. If the confidence is too low, the device could resort to traditional unlocking using swipe patterns or passwords. Other less security critical scenarios could use the user recognition to simplify the interface, e.g., showing a more basic menu or provide direct access to kids content without the need of unlocking when a child holds the device.

Multi-player games with handheld devices is another interesting area for social interaction in small groups. The tablet would show the game screen for the player who is holding the device. When the player passes the tablet to another player, the game screen adapts.

Zensei could also be integrated into electrical tools, such as power tools, garden tools, and kitchen appliances. These typically have defined ways of holding them, which helps robustness and accuracy, thanks to consistent alignment and contact. This could facilitate sharing tools in a workshop, where individual settings are restored when a user picks up the device. It could prevent use by children or people without necessary training. *Zensei* could also enable logging of professional tasks, e.g., lawn moving or woodworking, to quantify time for simplified billing and auditing.

FUTURE WORK

Zensei has a more physically complex setup compared to previous single-electrode sensing technologies (e.g., [39]). In the industry, single-piece injection-molded parts with integrated electronic circuit traces are widely used for mobile phone antennas and wireless charging coils. However, additive manufacturing techniques are becoming increasingly popular, and multi-material 3D printing, such as Autodesk's Project Wire [2], can 3D print plastic structures and conductive traces in a single process. We are interested in exploring these techniques for *Zensei* as well [18], to allow manufacturers to produce *Zensei*-equipped objects in small and large quantities.

In the implementation of *Zensei* used for our data analysis, the sensor hardware could only measure the absolute value of the phase difference due to the RF Amplitude/Phase detector IC's limitations. However, our latest sensor board, currently in testing, is capable of measuring the sign of the phase difference. This will enable *Zensei* to capture even more behavioral and physiological property data. We are interested in using this updated board for a much longer longitudinal data collection study and physically integrated with devices.

Zensei currently requires relatively demanding signal processing because of the amount of data collected by multiplexing between six electrodes in pairs. To address this, optimization-based electrode pair selection methods can be used to choose pairs that will yield the most useful information. As shown in our work, placement and number of electrodes is highly dependent on the device and expected usage. Furthermore, we plan to investigate how signal features on top of the raw data (e.g., maxima, minima, and inflection points) can help improve accuracy.

We also hope to explore how *Zensei* can operate in combination with other sensing technologies without compromising its transparent sensing. We are both interested in augmenting existing authentication devices that rely on contact (e.g., fingerprint sensors, keypads for pass codes), as well as adding sensors that can help *Zensei* assess the quality of measured samples. We believe that multimodal sensing and disambiguation can greatly boost the different scenarios where bioimpedance can be useful.

Lastly, there are situations in which users may want an explicit or obvious interaction for identification to maintain user privacy or understand the reason for certain customization behavior. For example, when tracking a guest user's behaviors on a new system that they may never return to again. Giving new users an option to be anonymous or explicitly identified is critical for user comfort.

CONCLUSIONS

We have introduced *Zensei*, a technique that allows objects to automatically recognize their user through wide-spectrum bioimpedance sensing. *Zensei's* sensing of the human body enables implicit personalization, individualization and adaptation without user instrumentation. We developed two versions of custom bioimpedance sensing hardware for our multi-electrode sensing system and, in particular, show a small credit-card-sized wireless sensor board. We implemented our technique in three form factors that were representative of our use cases of interest: a hand pad, smartphone, and chair.

Our large-scale and longitudinal data collection with 46 subjects using these form factors, and its associated evaluation and analysis, demonstrates promising results of $84.1\% \pm 5.0\%$ subject classification accuracy, in addition to a low false acceptance rate ($0.37\% \pm 0.10\%$). We have also analyzed and discussed how design parameters such as alignment, contact, electrode configuration and anatomy influence the different form factors. Our analysis of subject pool size and training data provides further insight into the potential of our technique.

We have demonstrated the feasibility of implementing our technique for smaller groups, such as families or work teams, where it can help to augment interaction with shared devices that would benefit from implicit personalization. We believe that *Zensei* has great potential in complementing other user sensing techniques, through its implicit sensing, the difficulty to steal or forge the signature, and its applicability to many different form factors, scales, and configurations.

We have also highlighted a set of applications related to the Internet of Things and ubiquitous computing, where we envision that *Zensei* could be integrated in, for example, door handles, kitchen appliances, furniture, vehicles, smart phones, and power tools, to make them smarter and user-aware. We hope that *Zensei* will inspire future techniques to enable more seamless and customized user interactions for a wide variety of objects and connected devices.

ACKNOWLEDGMENTS

REFERENCES

1. Apple. 2015. "About Touch ID security on iPhone and iPad". (2 November 2015). Retrieved September 18, 2016 from `https://support.apple.com/en-us/HT204587/`.

2. Autodesk. 2015. "Autodesk Wire". (5 January 2015). Retrieved September 18, 2016 from `https://spark.autodesk.com/blog/autodesk-and-voxel8-make-3d-printed-electronics-reality`.

3. Heribert Baldus, Steven Corroy, Alberto Fazzi, Karin Klabunde, and Tim Schenk. 2009. Human-centric connectivity enabled by body-coupled communications. *IEEE Commun. Mag.* 47, 6 (2009), 172–178. DOI:`http://dx.doi.org/10.1109/MCOM.2009.5116816`

4. Richard H Bayford. 2006. Bioimpedance tomography (electrical impedance tomography). *Annu. Rev. Biomed. Eng.* 8 (2006), 63–91. DOI:`http://dx.doi.org/10.1146/annurev.bioeng.8.061505.095716`

5. Debnath Bhattacharyya, Rahul Ranjan, Farkhod Alisherov A, and Minkyu Choi. 2009. Biometric Authentication : A Review. *Int. J. Serv. Sci. Technol.* 2, 3 (2009), 13–28.

6. Bojan Blažica, Daniel Vladušič, and Dunja Mladenić. 2013. MTi: A method for user identification for multitouch displays. *Int. J. Hum. Comput. Stud.* 71, 6 (June 2013), 691–702. DOI:`http://dx.doi.org/10.1016/j.ijhcs.2013.03.002`

7. Anja Bosy-Westphal, Sandra Danielzik, Ralf-Peter Dörhöfer, Wiebke Later, Sonja Wiese, and Manfred J Müller. 2006. Phase angle from bioelectrical impedance analysis: population reference values by age, sex, and body mass index. *J. Parenter. Enteral Nutr.* 30, 4 (2006), 309–16. DOI:`http://dx.doi.org/10.1177/0148607106030004309`

8. Daniel Buschek, Alexander De Luca, and Florian Alt. 2016. Evaluating the Influence of Targets and Hand Postures on Touch-based Behavioural Biometrics. In *Proc. CHI '16*. ACM, 1349–1361. DOI:`http://dx.doi.org/10.1145/2858036.2858165`

9. Margaret Cheney, David Isaacson, and Jonathan C Newell. 1999. Electrical impedance tomography. *SIAM review* 41, 1 (1999), 85–101. DOI:`http://dx.doi.org/10.1137/S0036144598333613`

10. Cory Cornelius. 2013. *Usable security for wireless body-area networks*. Ph.D. Dissertation. Dartmouth College. `http://dl.acm.org/citation.cfm?id=2604768`

11. Cory Cornelius and Christopher Gutierrez. 2014. A survey of biometrics for wearable devices. *Intel Technol. J.* 18, 4 (2014), 46–63. `http://libproxy.mit.edu/login?url=http://search.ebscohost.com/login.aspx?direct=true&db=aci&AN=97377853&site=eds-live`

12. Cory Cornelius, Ronald Peterson, Joseph Skinner, Ryan Halter, and David Kotz. 2014. A wearable system that knows who wears it. In *Proc. MobiSys '14*. ACM, 55–67. DOI:`http://dx.doi.org/10.1145/2594368.2594369`

13. Cory Cornelius, Jacob Sorber, Ronald Peterson, Joe Skinner, Ryan Halter, and David Kotz. 2012. Who wears me? bioimpedance as a passive biometric. In *Proc. HelthSec. '12*. 4.

14. Paul Dietz and Darren Leigh. 2001. DiamondTouch: a multi-user touch technology. In *Proc. UIST '01*. ACM, 219–226. DOI:`http://dx.doi.org/10.1145/502348.502389`

15. Dinei Florencio and Cormac Herley. 2007. A large-scale study of web password habits. In *Proc. 16th Int. Conf. World Wide Web - WWW '07*. 657–666. DOI:`http://dx.doi.org/10.1145/1242572.1242661`

16. Fortune. 2015. "Hackers have cracked more than 11 million Ashley Madison passwords". (11 September 2015). Retrieved September 18, 2016 from `http://fortune.com/2015/09/11/ashley-madison-passwords/`.

17. Kenneth R Foster and Henry C Lukaski. 1996. Whole-body impedance–what does it measure? *Am. J. Clin. Nutr.* 64, 3 Suppl (Sept. 1996), 388S–396S. `http://www.ncbi.nlm.nih.gov/pubmed/8780354`

18. Jörg Franke. 2014. *Three-dimensional molded interconnect devices (3D-MID) : materials, Manufacturing, assembly, and applications for injection molded circuit carrier*. Hanser Publications. DOI:`http://dx.doi.org/10.3139/9781569905524`

19. Davrondzhon Gafurov, Kirsi Helkala, and Torkjel Sø ndrol. 2006. Biometric gait authentication using accelerometer sensor. *J. Comput.* 1, 7 (2006), 51–59. DOI:`http://dx.doi.org/10.4304/jcp.1.7.51-59`

20. Anhong Guo, Robert Xiao, and Chris Harrison. 2015. CapAuth: Identifying and Differentiating User Handprints on Commodity Capacitive Touchscreens. In *Proc. ITS '15*. ACM, 59–62. DOI:`http://dx.doi.org/10.1145/2817721.2817722`

21. Chris Harrison, Munehiko Sato, and Ivan Poupyrev. 2012. Capacitive fingerprinting. In *Proc. UIST '12*. ACM, 537–543. DOI:`http://dx.doi.org/10.1145/2380116.2380183`

22. Eiji Hayashi and Jason Hong. 2011. A diary study of password usage in daily life. In *Proc. CHI '11*. ACM, 2627–2630. DOI:`http://dx.doi.org/10.1145/1978942.1979326`

23. Christian Holz and Patrick Baudisch. 2013. Fiberio: a touchscreen that senses fingerprints. In *Proc. UIST '13*. ACM, 41–50. DOI:`http://dx.doi.org/10.1145/2501988.2502021`

24. Christian Holz, Senaka Buthpitiya, and Marius Knaust. 2015. Bodyprint: Biometric User Identification on Mobile Devices Using the Capacitive Touchscreen to Scan Body Parts. In *Proc. CHI '15*. ACM, 3011–3014. DOI:`http://dx.doi.org/10.1145/2702123.2702518`

25. Christian Holz and Marius Knaust. 2015. Biometric Touch Sensing: Seamlessly Augmenting Each Touch with Continuous Authentication. In *Proc. UIST '15*. ACM, 303–312. DOI: http://dx.doi.org/10.1145/2807442.2807458

26. Tyna A Hope and Siân E Iles. 2004. Technology review: the use of electrical impedance scanning in the detection of breast cancer. *Breast Cancer Res.* 6, 2 (2004), 69–74. DOI:http://dx.doi.org/10.1186/bcr744

27. Anil K Jain, Arun Ross, and Salil Prabhakar. 2004. An Introduction to Biometric Recognition. *IEEE Trans. Circuits Syst. Video Technol.* 14, 1 (2004), 4–20. DOI: http://dx.doi.org/10.1109/TCSVT.2003.818349

28. Jawbone. 2014. "Jawbone UP3". (4 November 2014). Retrieved September 18, 2016 from https://jawbone.com/store/buy/up3.

29. Paul Kry and Dinesh Pai. 2006. Grasp Recognition and Manipulation with the Tango. In *10th Int. Symp. Exp. Robot.*, Vol. 39. Springer, 551–559. DOI: http://dx.doi.org/10.1007/978-3-540-77457-0_52

30. Kin Fong Lei, Kuan Hao Chen, Po Hsiang Tsui, and Ngan Ming Tsang. 2013. Real-Time Electrical Impedimetric Monitoring of Blood Coagulation Process under Temperature and Hematocrit Variations Conducted in a Microfluidic Chip. *PLoS One* 8, 10 (2013). DOI: http://dx.doi.org/10.1371/journal.pone.0076243

31. Vadim F. Lvovich. 2012. *Impedance Spectroscopy: Applications to Electrochemical and Dielectric Phenomena*. John Wiley and Sons.

32. Kent Lyons, Seung Wook Kim, Shigeyuki Seko, David Nguyen, Audrey Desjardins, Mélodie Vidal, David Dobbelstein, and Jeremy Rubin. 2014. Loupe: a handheld near-eye display. In *Proc. UIST '14*. ACM, 351–354. DOI:http://dx.doi.org/10.1145/2642918.2647361

33. Philipp Mock, Jörg Edelmann, Andreas Schilling, and Wolfgang Rosenstiel. 2014. User identification using raw sensor data from typing on interactive displays. In *Proc. IUI '14*. ACM, 67–72. DOI: http://dx.doi.org/10.1145/2557500.2557503

34. E Rehmi Post, Matt Reynolds, Matthew Gray, Joe Paradiso, and Neil Gershenfeld. 1997. Intrabody buses for data and power. *Dig. Pap. First Int. Symp. Wearable Comput.* (1997), 52–55. DOI: http://dx.doi.org/10.1109/ISWC.1997.629919

35. Kasper B Rasmussen, Marc Roeschlin, Ivan Martinovic, and Gene Tsudik. 2014. Authentication Using Pulse-Response Biometrics. In *Proc. NDSS '14*. DOI: http://dx.doi.org/10.14722/ndss.2014.23208

36. Jun Rekimoto. 2002. SmartSkin: an infrastructure for freehand manipulation on interactive surfaces. In *Proc. CHI '02*. ACM, 113–120. DOI: http://dx.doi.org/10.1145/503376.503397

37. Samsung. 2014. "Samsung Simband: Samsung's concept of what a digital health devices should be". (28 May 2014). Retrieved September 18, 2016 from https://www.simband.io/.

38. T Scott Saponas, Chris Harrison, and Hrvoje Benko. 2011. PocketTouch: Through-fabric capacitive touch input. In *Proc. UIST '11*. ACM, 303–307. DOI: http://dx.doi.org/10.1145/2047196.2047235

39. Munehiko Sato, Ivan Poupyrev, and Chris Harrison. 2012. Touché: enhancing touch interaction on humans, screens, liquids, and everyday objects. In *Proc. CHI '12*. ACM, 483–492. DOI: http://dx.doi.org/10.1145/2207676.2207743

40. Stefan Schneegass, Youssef Oualil, and Andreas Bulling. 2016. SkullConduct: Biometric User Identification on Eyewear Computers Using Bone Conduction Through the Skull. In *Proc. CHI '16*. ACM, 1379–1384. DOI: http://dx.doi.org/10.1145/2858036.2858152

41. Shimmer. 2016. "Shimmer Sensing". (18 September 2016). Retrieved September 18, 2016 from http://www.shimmersensing.com/.

42. Hyunyoung Song, Hrvoje Benko, Francois Guimbretiere, Shahram Izadi, Xiang Cao, and Ken Hinckley. 2011. Grips and gestures on a multi-touch pen. In *Proc. CHI '11*. ACM, 1323–1332. DOI: http://dx.doi.org/10.1145/1978942.1979138

43. Sony. 2015. "Sony Xperia Z5". (2 September 2015). Retrieved September 18, 2016 from http://www.sonymobile.com/global-en/products/phones/xperia-z5.

44. Kenji Suzuki, Taku Hachisu, and Kazuki Iida. 2016. EnhancedTouch: A Smart Bracelet for Enhancing Human-Human Physical Touch. In *Proc. CHI '16*. ACM, 1282–1293. DOI: http://dx.doi.org/10.1145/2858036.2858439

45. Brandon T Taylor and V Michael Bove. 2008. The bar of soap: a grasp recognition system implemented in a multi-functional handheld device. In *Proc. CHI '08*. ACM, 3459–3464. DOI: http://dx.doi.org/10.1145/1358628.1358874

46. Brandon T Taylor and V Michael Bove. 2009. Graspables: Grasp-Recognition as a User Interface. In *Proc. CHI '09*. ACM, 917–925. DOI: http://dx.doi.org/10.1145/1518701.1518842

47. J. A. Unar, Woo Chaw Seng, and Almas Abbasi. 2014. A review of biometric technology along with trends and prospects. *Pattern Recognit.* 47, 8 (2014), 2673–2688. DOI:http://dx.doi.org/10.1016/j.patcog.2014.01.016

48. Nicolas Villar, Xiang Cao, Billy Chen, Shahram Izadi, Dan Rosenfeld, Hrvoje Benko, John Helmes, Jonathan Westhues, Steve Hodges, Eyal Ofek, and Alex Butler. 2009. Mouse 2.0: Multi-touch meets the mouse.. In *Proc. UIST '09*. ACM, 33–42. DOI: http://dx.doi.org/10.1145/1622176.1622184

49. Weka. 2016. "Weka Toolkit". (18 September 2016). Retrieved September 18, 2016 from http://www.cs.waikato.ac.nz/ml/weka/.

50. Roman V. Yampolskiy and Venu Govindaraju. 2008. Behavioural biometrics: a survey and classification. *Int. J. Biom.* 1, 1 (June 2008), 81–132. DOI: http://dx.doi.org/10.1504/IJBM.2008.018665

51. Yang Zhang and Chris Harrison. 2015. Tomo: Wearable, Low-Cost Electrical Impedance Tomography for Hand Gesture Recognition. In *Proc. UIST '15*. ACM, 167–173. DOI:http://dx.doi.org/10.1145/2807442.2807480

52. Yang Zhang, Junhan Zhou, Gierad Laput, and Chris Harrison. 2016. SkinTrack: Using the Body As an Electrical Waveguide for Continuous Finger Tracking on the Skin. In *Proc. CHI '16*. ACM, 1491–1503. DOI: http://dx.doi.org/10.1145/2858036.2858082

53. Nan Zheng, Kun Bai, Hai Huang, and Haining Wang. 2014. You Are How You Touch: User Verification on Smartphones via Tapping Behaviors. In *Proc. IEEE Int. Conf. Netw. Protoc. '14*. IEEE, 221–232. DOI: http://dx.doi.org/10.1109/ICNP.2014.43

54. Thomas G Zimmerman. 1996. Personal Area Networks: Near-field intrabody communication. *IBM Syst. J.* 35, 3.4 (sep 1996), 609–617. DOI: http://dx.doi.org/10.1147/sj.353.0609

55. Thomas G Zimmerman, Joshua R Smith, Joseph A Paradiso, David Allport, and Neil Gershenfeld. 1995. Applying electric field sensing to human-computer interfaces. *Proc. CHI '95* (May 1995), 280–287. DOI: http://dx.doi.org/10.1145/223904.223940
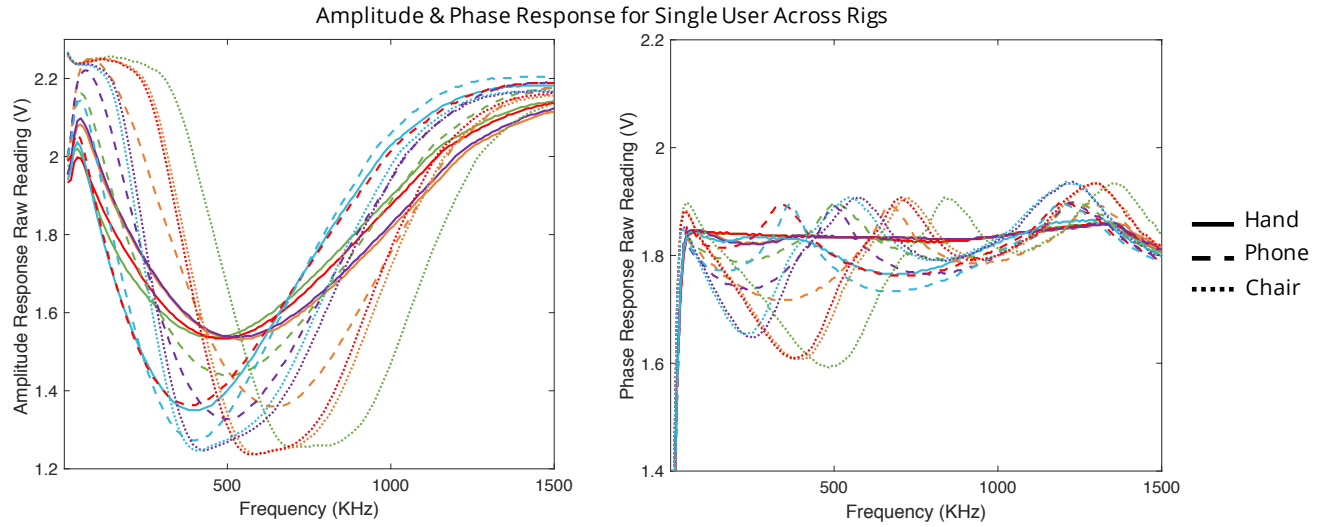
APPENDIX
Raw Data Demonstration

Figure 18. A single user's amplitude and phase response for the *Hand Pad*, *Smartphone*, and *Chair* rigs (denoted by solid, dashed, and dotted lines, respectively). Colors correspond to the electrodes shown in Figure 4 .
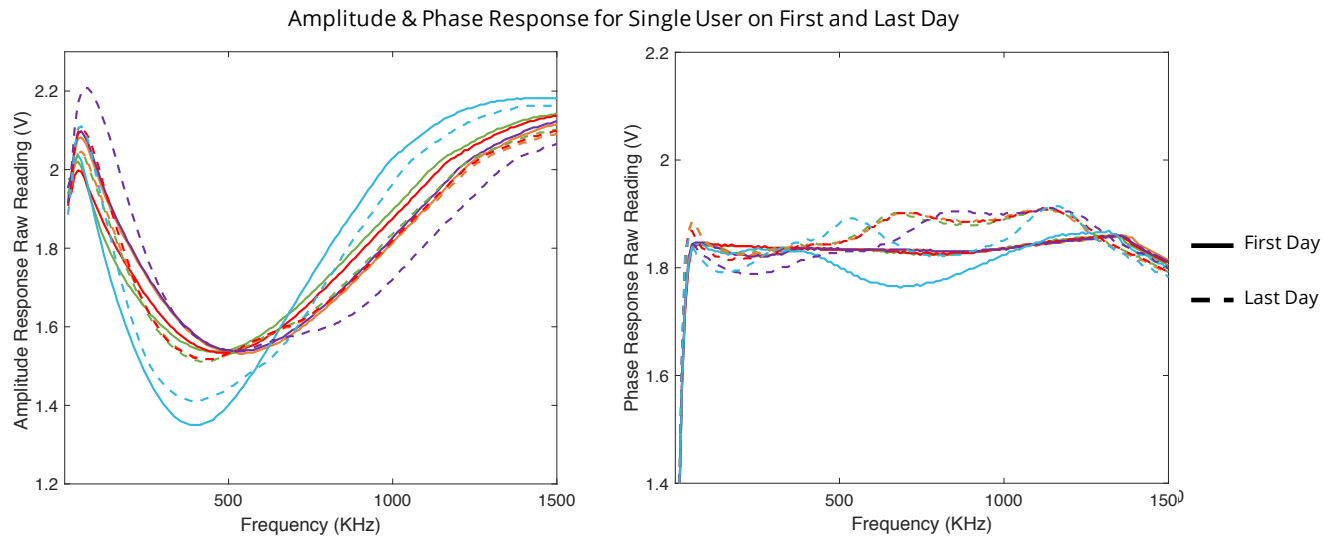

Figure 19. A single user's amplitude and phase response on the first and last days of the data collection period (denoted by solid and dashed lines, respectively). Colors correspond to the electrodes shown in Figure 4.
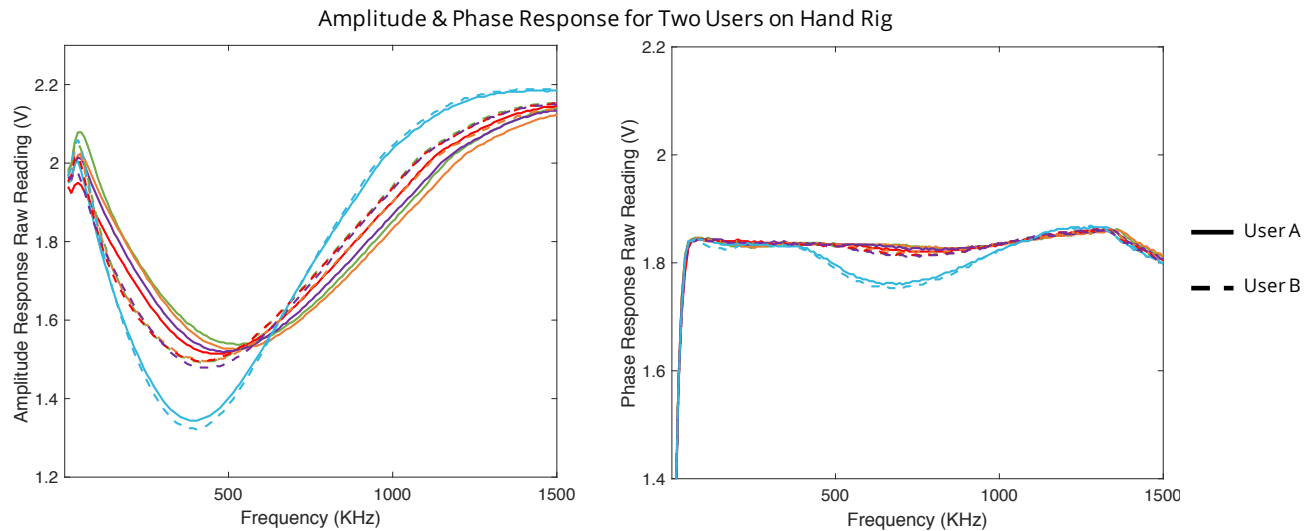

Figure 20. Two different users' amplitude and phase response on the hand rig (Users A and B are denoted by solid and dashed lines, respectively). Colors correspond to the electrodes shown in Figure 4.